

Comparing Solutions to the Nonlinear Dissipative Wave Equation

Zaki Mrzog Alaofi^{1,2}, Talaat Sayed El-Danaf³, Silvestru Sever Dragomir²

¹Department of Mathematics, College of Science and Arts, King Khalid University, Muhayil Asir, KSA

²Mathematics, College of Engineering & Science, Victoria University, Melbourne, Australia

³Department of Mathematics, Faculty of Sciences and Arts, Taibah University, Medina, KSA

Email: zaki.alaofi@live.vu.edu.au, zaleawfi@kku.edu.sa, tdanaf@taibahu.edu.sa, sever.dragomir@vu.edu.au

How to cite this paper: Alaofi, Z.M., El-Danaf, T.S. and Dragomir, S.S. (2022) Comparing Solutions to the Nonlinear Dissipative Wave Equation. *Journal of Applied Mathematics and Physics*, 10, 1281-1296. <https://doi.org/10.4236/jamp.2022.104090>

Received: March 8, 2022

Accepted: April 24, 2022

Published: April 27, 2022

Copyright © 2022 by author(s) and Scientific Research Publishing Inc. This work is licensed under the Creative Commons Attribution International License (CC BY 4.0). <http://creativecommons.org/licenses/by/4.0/>



Open Access

Abstract

In previous decades, many of the practical problems arising in scientific fields such as physics, engineering, and mathematics have been related to nonlinear fractional partial differential equations. One of these nonlinear partial differential equations, the dissipative wave equation, has been found to have a plethora of useful applications in different fields. A special class of solutions has been studied for the dissipative wave equation including exact solutions and approximate solutions. The aim of this article is to compare the non-polynomial spline method and the cubic B-spline method with the solution of a nonlinear dissipative wave equation. We will conduct a comparison of the stability of the two methods using the Von Neumann stability analysis. In addition, a numerical example will be presented to illustrate the accuracy of these methods.

Keywords

Dissipative Wave Equation, Cubic B-Spline, Non-Polynomial Spline, Truncation Error, Von Neumann Stability

1. Introduction

Nonlinear partial differential equations (NPDEs) are encountered in various fields such as physics, chemistry, biology, mathematics and engineering. Most nonlinear models of real-life problems are still proving difficult to solve either numerically or theoretically. Recently, much attention has been devoted to the search for better and more efficient solution methods for determining a solution, approximate or exact, analytical or numerical, for nonlinear models [1].

Many methods have been developed to solve a dissipative wave equation, in-

cluding the non-polynomial spline method and the cubic B-spline method. Researchers who have used the non-polynomial spline method include El-Danaf and Faisal (2009), who used a non-polynomial spline-based method to obtain numerical solutions for a dissipative wave equation. The developed method was shown to be conditionally stable for the given values of specified parameters. Furthermore, the obtained numerical results reveal that their proposed method maintains good accuracy [2]. Zaki Ahmed *et al.* (2020) used a non-polynomial spline function to obtain numerical solutions for a dissipative wave equation at middle points for lattice in space direction and at the same time. The presented method was shown to be conditionally stable. In addition, the computational results revealed that their proposed technique was suitable for the solution of these equations and agreed with the true solutions [3]. The cubic B-spline has been employed by many researchers to solve nonlinear dissipative wave equations. The most recent relevant results are those presented by Alaofi *et al.* in 2021. The stability analysis investigation demonstrated that the method is conditionally stable. The developed method is shown to be conditionally stable for given values of specified parameters. The obtained numerical results indicate that the proposed method maintains good accuracy [4]. As the previous two methods, non-polynomial spline and cubic B-spline, have been used many times in recent years, we wanted to present a comparison between them to assist future researchers. Section one outlines some previous studies on the nonlinear dissipative wave equation. Section two offers basic definitions and descriptions of the non-polynomial spline functions, local truncation errors, and the cubic B-spline method. The third section will describe the stability analysis. Using the concept of stability and the von Neumann method, three stability-related cases are provided. Section four addresses numerical illustration. In this section, we offer an example from each author as well as their results. We have also presented additional results that we have obtained during our research. In the final section, we offer some conclusions and highlight some areas for further development.

The generalised nonlinear dissipative wave equation of the form [5]:

$$\frac{\partial^2 u}{\partial t^2} - \frac{\partial^2 u}{\partial x^2} + 2u_t u = g(x, t) \quad (1)$$

under the boundary conditions:

$$u(a, t) = \eta_1, \quad u(b, t) = \eta_2, \quad t \geq 0 \quad (2)$$

and initial conditions:

$$u(x, 0) = f_1(x), \quad u_t(x, 0) = f_2(x), \quad a \leq x \leq b \quad (3)$$

2. The Methods

In this section, we will illustrate the non-polynomial spline method and the cubic B-spline method.

2.1. Non-Polynomial Spline Method

The Non-polynomial Spline Functions [6]

Let $a = x_0 < x_1 < \dots < x_N = b$ be a subdivision of the interval $[a, b]$. The non-polynomial spline function is defined by

$$p(x, t_n) = \begin{cases} p_0(x, t_n), x \in [x_0, x_1] \\ p_1(x, t_n), x \in [x_1, x_2] \\ \vdots \\ p_{N-1}(x, t_n), x \in [x_{N-1}, x_N] \end{cases}$$

where $p_j(x, t_n)$ is a mixed spline function of the form:

$$p_j(x, t_n) = b_{1j}(t_n) \cos \omega(x - x_j) + b_{2j}(t_n) \sin \omega(x - x_j) + a_{1j}(t_n)(x - x_j)^r + a_{2j}(t_n)(x - x_j)^{r-1} + \dots + a_{rj}(t_n)(x - x_j) + a_{(r+1)j}(t_n), j = 0, 1, \dots, N-1.$$

and r represents the degree of the polynomial part.

Remark

We can use other functions as $(\cosh \omega x, \sinh \omega x)$, $(\tanh \omega x, \operatorname{sech} \omega x)$, $(\cosh \omega x, \operatorname{sech} \omega x)$ and $(e^{\omega x}, e^{-\omega x})$ instead of $(\cos \omega x, \sin \omega x)$ in $p_j(x, t_n)$.

Local truncation error [6]

The truncation error is the difference between the differential equation and its approximating difference equation. Let $F_{jn}(u) = 0$ represent the differential equation at the $(j, n)_{th}$ mesh point. If u is replaced by U at the mesh points of the difference equation, then the value of $F_{jn}(U)$ is named the local truncation error at the $(j, n)_{th}$ mesh point. We denote it by T_j^n .

Zaki Ahmed [3] et al. and El-Danaf [2] et al. used the non-polynomial spline method.

To set up the non-polynomial spline method, select an integer $N > 0$ and time-step size $k > 0$. With $h = \frac{b-a}{N+1}$, the mesh points (x_i, t_j) are:

$$x_i = a + ih, \text{ for each } i = 0, 1, \dots, N+1$$

and,

$$t_j = jk, \text{ for each } j = 0, 1, \dots$$

Let $Z_i^j \equiv Z(x_i, t_j)$ be an approximation to $u(x_i, t_j)$, obtained by the segment $P_i(x, t_j)$ of the mixed spline function passing through the points (x_i, Z_i^j) and (x_{i+1}, Z_{i+1}^j) . Each segment has the forms (4) and (5) as follows:

Zaki Ahmed et al. used the following form,

$$Q_i(x, t_j) = a_i(t_j) \cos w(x - x_i) + b_i(t_j) \sin w(x - x_i) + c_i(t_j) \quad (4)$$

El-Danaf et al. used the following form,

$$P_i(x, t_j) = a_i(t_j) \cos \omega(x - x_i) + b_i(t_j) \sin \omega(x - x_i) + c_i(t_j)(x - x_i) + d_i(t_j) \quad (5)$$

where $i = 0, 1, \dots, n-1$; $j = 0, 1, \dots$; $a_i(t_j)$; $b_i(t_j)$; $c_i(t_j)$ and $d_i(t_j)$ are unknowns to be determined and ω is a parameter of the trigonometric functions.

The truncation error for Equation (4) at $i = 1, n$ is as follows:

$$t_i^j = \left[\left(\frac{6}{8} - (w_0 + w_1 + w_2 + w_3) \right) h^2 D_x^2 + \left(\frac{1}{2} - \left(\frac{w_0 + 3w_1 + 5w_2 + 7w_3}{2} \right) \right) h^3 D_x^3 \right. \\ \left. + \left(\frac{39}{192} - \left(\frac{w_0 + 9w_1 + 25w_2 + 49w_3}{8} \right) \right) h^4 D_x^4 \right. \\ \left. + \left(\frac{1}{16} - \left(\frac{w_0 + 27w_1 + 125w_2 + 343w_3}{48} \right) \right) h^5 D_x^5 \right. \\ \left. + \left(\frac{726}{46080} - \left(\frac{w_0 + 81w_1 + 625w_2 + 2401w_3}{384} \right) \right) h^6 D_x^6 + \dots \right] u_i^j$$

to make $t_i^j, i = 1, n$ of order $O(h^6)$.

The approximation with local truncation error of $O(k^2)$:

$$Z_i^1 \approx Z_i^0 + kf_2(x_i) + \frac{k^2}{2} \left(g_i^0 + \frac{d^2 f_1}{dx^2}(x_i) - 2f_2 f_1 \right), \quad i = 1, \dots, N.$$

2.2. The Cubic B-Spline Method

The cubic B-spline functions $\{\phi_i(x)\}$ are defined by:

$$\phi_i(x) = \frac{1}{h^3} \begin{cases} (x - x_{i-2})^3 & x \in [x_{i-2}, x_{i-1}] \\ h^3 + 3h^2(x - x_{i-1}) + 3h(x - x_{i-1})^2 - 3(x - x_{i-1})^3 & x \in [x_{i-1}, x_i] \\ h^3 + 3h^2(x_{i+1} - x) + 3h(x_{i+1} - x)^2 - 3(x_{i+1} - x)^3 & x \in [x_i, x_{i+1}] \\ (x_{i+2} - x)^3 & x \in [x_{i+1}, x_{i+2}] \\ 0 & \text{otherwise} \end{cases}$$

where $h = x_{i+1} - x_i, i = 0, 1, \dots, N-1$. The values of the cubic B-spline $\phi_i(x)$ and its first and second derivatives vanish outside the interval (x_{i-2}, x_{i+2}) . We establish the values of $\phi_i(x)$ and its derivatives at the knots in **Table 1**.

This type of spline is used to obtain an approximate solution to partial differential equations, see [4].

The Analysis and the Initial State for the Dissipative Wave Equation

1) The approximate solution of the dissipative wave equation is considered to be:

$$U_N(x, t) = \sum_{i=0}^n w_i(t_j) \phi_i(x_j) \\ = \sum_{i=-1}^{N+1} [\omega_i^{n-1} - 2\omega_i^n + \omega_i^{n+1}] \phi_i(x_j) - k^2 \sum_{i=-1}^{N+1} \omega_i(t) \phi_i''(x_j) \\ + k^2 [\omega_i^{n+1} + \omega_i^{n-1}] \phi_i(x_j) \sum_{\delta=-1}^{N+1} \frac{d\omega_\delta(t)}{dt} \phi_\delta(x_j) \\ = k^2 \eta_j^n(x, t)$$

Table 1. The values of $\phi_i(x)$ and its derivatives with knots at the shown points.

x	x_{i-2}	x_{i-1}	x_i	x_{i+1}	x_{i+2}
$\phi_i(x)$	0	1	4	1	0
$\phi_i'(x)$	0	$3/h$	0	$-3/h$	0
$\phi_i''(x)$	0	$6/h^2$	$-12/h^2$	$6/h^2$	0

where $\phi_i(x_j)$ represents the spline functions, and $w_i(t_j)$ represents the unknowns to be determined.

2) The dissipative wave equation reduced to system of ODE.

They get:

$$\begin{aligned} & a_i \omega_{i-1}^{n+1} + b_i \omega_i^{n+1} + c_i \omega_{i+1}^{n+1} \\ & = -d_i \omega_{i-1}^n - e_i \omega_i^n - f_i \omega_{i+1}^n - n_i \omega_{i-1}^{n-1} - s_i \omega_i^{n-1} - l_i \omega_{i+1}^{n-1} + k^2 \eta_i^n(x, t) \end{aligned}$$

3) Using the boundary conditions to get $N+3$ equations in $N+3$ unknowns.

$$\begin{aligned} & \frac{6}{h^2} \omega_{-1} - \frac{12}{h^2} \omega_0 + \frac{6}{h^2} \omega_1 = 0, \\ & \frac{6}{h^2} \omega_{N-1} - \frac{12}{h^2} \omega_N + \frac{6}{h^2} \omega_{N+1} = 0. \end{aligned}$$

4) Apply the initial conditions to get the independent variables:

$$(\omega_{-1}^0, \omega_0^0, \dots, \omega_N^0, \omega_{N+1}^0)^T$$

5) After getting the following system of algebraic equations:

$$A\omega^{n+1} = -B\omega^n - C\omega^{n-1} + k^2 \eta^n(x, t)$$

6) Two initial conditions are applied to get the following system:

$$\omega_{i-1}^0 + 4\omega_i^0 + \omega_{i+1}^0 = u(x_j, 0), \quad j = 0, 1, 2, \dots, N$$

7) Adding the following two initial conditions to complete the system of equations:

$$\begin{aligned} & -3\omega_{-1}^0 + 3\omega_1^0 = hu_x(a, 0) \\ & -3\omega_{N-1}^0 + 3\omega_{N+1}^0 = hu_x(b, 0) \end{aligned}$$

3. The Stability Analysis

Stability [7]

Suppose that, in a computation involving a difference scheme, an error ξ^0 is introduced at a time level t^0 , and suppose that no further errors occur. If ξ^n denotes the error resulting from this error at time t^n , then the scheme is stable if $|\xi^n|$ remains bounded as $n \rightarrow \infty$ (i.e., the error must not grow without limit).

Stability by the Fourier series method (Von Neumann's Method) [7]

This method, developed by Von Neumann during World War II, was first discussed in detail by O'Brien, Hyman and Kaplan in a paper published in 1951. It expresses an initial line of errors in terms of a finite Fourier series, and considers the growth of a function that reduces to this series for $t=0$ using a "variables separable" method identical to that commonly used for deriving analytical solutions to partial differential equations. If we write $N_j^n = u_j^n + \xi_j^n$ in the difference scheme, and if it is linear, then ξ^n will satisfy the same equation as u_j^n expresses the error as a finite Fourier series of the form $\sum \xi^n(t) e^{ikx_j}$. Fur-

thermore, if the equation is linear, then we need consider only the growth of a single form:

$$\xi_j^n = \xi^n e^{ikx_j},$$

where $i = \sqrt{-1}$, and let:

$$g = \frac{\xi^{n+1}}{\xi^n},$$

where g is called the growth of an amplification factor. For stability, the Von Neumann condition requires:

$$|g| \leq 1 + O(\Delta t).$$

i.e. the error will not increase as t increases.

It should be noted that this method applies only to linear difference equations with periodic initial data. The criterion $|g| \leq 1$ is necessary and sufficient for three or more level equations—though it is always necessary. In practice, the method often gives useful results even when its application is not fully justified.

According to the Von Neumann technique we have:

$$S_i^j = \xi^j e^{(q\phi hi)} \quad (6)$$

where $q^2 = -1$, ϕ is the mode number, h is the element size, and ξ is the amplification factor.

For stability, we must have $|\xi_{\pm}| \leq 1$. Also, from Equation (6) we can observe that the product of the two values of ξ is clearly unity. So, three cases arise.

Case 1: Both the roots are equal to unity. In this case, the discriminant of the quadratic Equation (6) is zero.

Case 2: One of the roots is greater than unity. In this case, the discriminant is greater than zero. This means the stability condition, that is $|\xi_{\pm}| \leq 1$, is not satisfied. In other words, ξ^j would grow in an unbounded manner.

Case 3: The discriminant is less than zero, that is: $\mu^2 - 1 < 0$. Thus, for stability:

$$-1 \leq \mu \leq 1 \quad (7)$$

[2] and [3] using Equation (6), the above inequality becomes:

$$-\frac{k^2 d^*}{2} \leq \frac{2k^2 \sin^2(\phi/2)}{(\beta + 2\alpha) - 4\alpha \sin^2(\phi/2)} \leq 2 - \frac{k^2 d^*}{2} \quad (8)$$

Two cases will be discussed:

Case 1: For $\beta = -2\alpha$, inequality (8) becomes:

$$-\frac{k^2 d^*}{2} \leq \frac{k^2}{-2\alpha} \leq 2 - \frac{k^2 d^*}{2}$$

We can say that our system is stable for $\beta = -2\alpha$, $\alpha < 0$, and $k^2 \ll |\alpha|$ such that $|\alpha|$, and k^2 are small enough.

Case 2: For $\alpha > 0$, $\beta > 2\alpha$, the quantity $(\beta + 2\alpha) - 4\alpha \sin^2(\phi/2)$ is positive, so we can say that stability in this case requires $\alpha > 0$, $\beta > 0$, and $\beta > 2\alpha$

such that α, β and $k^2 \ll \beta$ are small enough and $\sin(\phi/2) \neq 0$.

On the other hand, [4] using Equation (6), the (7) inequality becomes:

$$-1 \leq \frac{[(-2-r_1)\cos\phi h + (-4+r_1)]}{[(2+2k^2m)\cos\phi h + (4+4k^2m)]} \leq 1. \quad (9)$$

After simplifying inequality (9), we get:

$$\left(\frac{-mh^2}{3} + 1\right) + \left(\frac{2mh^2}{3} - 2\right) \sin^2 \frac{\phi h}{2} \leq \left(1 + \frac{2mh^2}{3}\right),$$

If h is small enough, the method is conditionally stable.

4. Numerical Illustration

Example. Consider the dissipative wave equation [8]:

$$\frac{\partial^2 u}{\partial t^2} - \frac{\partial^2 u}{\partial x^2} + 2u_t u = -2\sin^2 x \sin t \cos t \leq x \leq \pi, \quad t \geq 0, \quad (10)$$

with the initial conditions:

$$u(x, 0) = \sin x, \quad u_t(x, 0) = 0, \quad (11)$$

and the boundary conditions:

$$u(0, t) = u(\pi, t) = 0. \quad (12)$$

4.1. The Results of [2]

Table 2 shows maximum error occurred at 0.5, 1.5, 2.5, and 3.5 respectively. Numerical values have been computed using the non-polynomial spline method and reported in **Table 3** & **Table 4**. The simulation is done up to $x = 0.8\pi$. We

Table 2. The L_∞ error for the numerical and exact solutions when $k = 0.01$, $h = \frac{\pi}{40}$, $\alpha = -1.01$; $\beta = -2\alpha$.

Time	0.5	1.5	2.5	3.5
L_∞ error	2.55058×10^{-4}	1.76001×10^{-3}	3.21326×10^{-3}	4.25842×10^{-3}

Table 3. Comparison between the numerical and exact solutions at $h = \pi/40$; $t = 1.5$; $\alpha = 2 \times 10^{-7}$; $\beta = 6.18 \times 10^{-3}$.

x	Exact solution	Numerical solution
0.2π	0.04157828392871431	0.041764024258423134
0.3π	0.05722759828369953	0.057475017088467340
0.4π	0.06727507659055325	0.067547692975227380
0.5π	0.07073720166770290	0.071012934346015150
0.6π	0.06727507659055325	0.067547692975153300
0.7π	0.05722759828369953	0.057475017088395690
0.8π	0.04157828392871431	0.041764024258327160

can conclude that applying nonpolynomial splines in the solution of partial differential equations is a promising approach.

4.2. The Results of [3]

L_∞ error norms are reported in **Table 5**. In addition, comparisons of approximate and exact solutions at different nodes x and different time levels are reported in **Table 6** & **Table 7**.

The relation between time and the maximum error is shown in **Figure 1** and

Table 4. Comparison between the numerical and exact solutions at $h = \pi/40$; $t = 2.5$; $\alpha = 2 \times 10^{-7}$; $\beta = 6.18 \times 10^{-3}$.

x	Exact solution	Numerical solution
0.2π	-0.47090040218675855	-0.47064203333751690
0.3π	-0.64813879991245870	-0.64771280914059780
0.4π	-0.76193285605417060	-0.76136720198110770
0.5π	-0.80114361554693370	-0.80052412271783310
0.6π	-0.76193285605417060	-0.76136720198119200
0.7π	-0.64813879991245870	-0.64771280914063270
0.8π	-0.47090040218675855	-0.47064203333747706

Table 5. The maximum absolute errors at $h = \frac{\pi}{50}$, $k = 0.01$, $\alpha = -1$ and $\beta = -2\alpha$.

Time	0.5	1.0	1.5	2.0
L_∞ error	8.7356×10^{-4}	2.5274×10^{-3}	4.4852×10^{-3}	7.5875×10^{-3}

Table 6. The true and numerical solution at $h = \frac{\pi}{50}$, $k = 0.001$, $t = 0.25$, $\alpha = 10^{-5}$ and $\beta = 0.005$.

x	True solution	Numerical solution
0.07π	0.211415560113106	0.212781989904912
0.17π	0.493342243118144	0.496403435602516
0.27π	0.726977150049252	0.731322133816448
0.37π	0.889450468385897	0.894631106006615
0.47π	0.964858177711116	0.970411644544139
0.57π	0.945818846039751	0.951279053551595
0.67π	0.834196175810620	0.839097661902968
0.77π	0.640916571706624	0.644800283101537
0.87π	0.384899588035650	0.387329859409562
0.97π	0.091205950934626	0.091795241347949

Table 7. The true and numerical solution at $h = \frac{\pi}{50}$, $k = 0.01$, $t = 2.5$, $\alpha = -1$ and $\beta = -2\alpha$.

x	True solution	Numerical solution
0.07π	-0.173449822213779	-0.173880443622743
0.17π	-0.404748469382337	-0.407480685897835
0.27π	-0.596427516319343	-0.603406828812836
0.37π	-0.729724082404153	-0.741447604522964
0.47π	-0.791590171016600	-0.806147786803187
0.57π	-0.775969898356912	-0.789769859046287
0.67π	-0.684392285545858	-0.694307145831281
0.77π	-0.525821587384132	-0.530927685708137
0.87π	-0.315779808634822	-0.317328698954233
0.97π	-0.074827302049036	-0.074921135704477

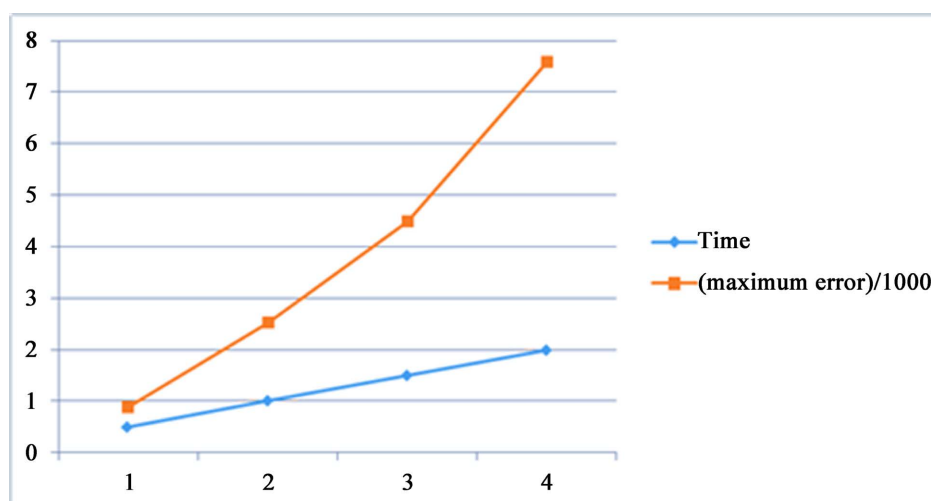


Figure 1. The relation between time and maximum error as per Table 5.

the graph of exact and approximate solutions for different time levels are depicted in Figure 2.

4.3. The Results of [4]

To make a comparison quantitatively, they have computed the error norms L_∞ in Table 8. Moreover, the comparison of obtained numerical results with the cubic B-spline method is presented in Table 9 & Table 10 when $t = 0.2$ and $t = 2$.

Figure 3 & Figure 4 depict a comparison of exact and approximate solutions when $t = 2$ and $t = 5$.

In the following section, we introduce the numerical results, which have been obtained by [4].

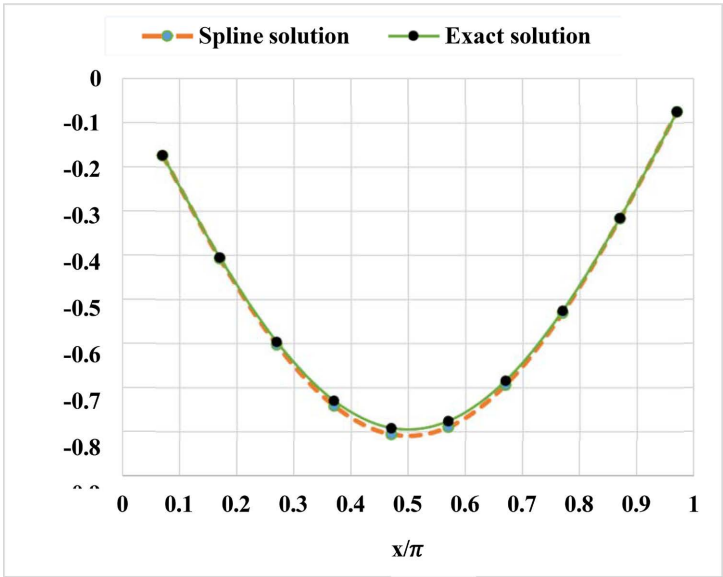


Figure 2. The true solution (green) and numerical solution (red) at $h = \frac{\pi}{50}$, $k = 0.01$, $\alpha = -1$, $\beta = -2\alpha$ and $t = 2.5$.

Table 8. The L_∞ error for the numerical and exact solutions when $k = 0.01$, $h = \frac{\pi}{20}$ from $t = 0.5$ to $t = 2.0$.

Time	0.5	1.0	1.5	2.0
L_∞ error	6.2131×10^{-4}	6.2454×10^{-4}	1.92996×10^{-3}	3.87406×10^{-3}

Table 9. Comparison between the numerical and exact solutions at $t = 0.2$, $k = 0.002$, $h = \frac{\pi}{20}$.

x	Numerical Solution	Exact Solution
0.1π	0.302857	0.303116
0.2π	0.576069	0.576509
0.3π	0.792891	0.793442
0.4π	0.932099	0.932707
0.5π	0.980067	0.980692
0.6π	0.932099	0.932707
0.7π	0.792891	0.793442
0.8π	0.576069	0.576509
0.9π	0.302857	0.303116

4.4. Our Results

In **Table 11**, the computational maximum errors with respect to the exact solution and numerical solution.

Table 10. Comparison between the numerical and exact solutions at $t = 2$, $k = 0.002$, $h = \frac{\pi}{20}$.

x	Numerical Solution	Exact Solution
0.1π	-0.128596	-0.129169
0.2π	-0.244605	-0.245756
0.3π	-0.33667	-0.338348
0.4π	-0.395779	-0.397833
0.5π	-0.416147	-0.418337
0.6π	-0.395779	-0.397833
0.7π	-0.33667	-0.338348
0.8π	-0.244605	-0.245756
0.9π	-0.128596	-0.129169

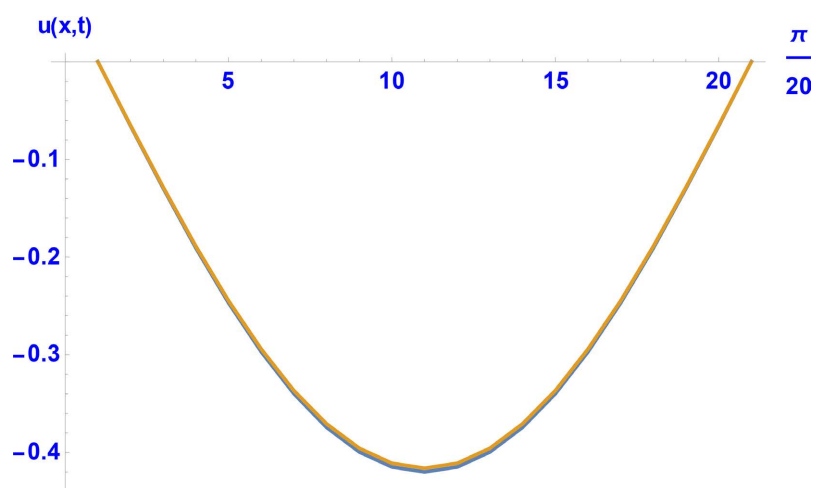


Figure 3. The exact and numerical results when the time $t = 2.0$ with $k = 0.01$.



Figure 4. The exact and numerical results when the time $t = 5.0$ with $k = 0.01$.

Table 11. The L_∞ error for the numerical and exact solutions for a big time when $k = 0.01$, $h = \frac{\pi}{20}$ from $t = 15.0$ to $t = 50.0$.

Time	15.0	25.0	35.0	45.0	50.0
L_∞ error	2.5282×10^{-2}	6.1599×10^{-2}	4.3337×10^{-2}	2.3355×10^{-2}	2.2784×10^{-2}

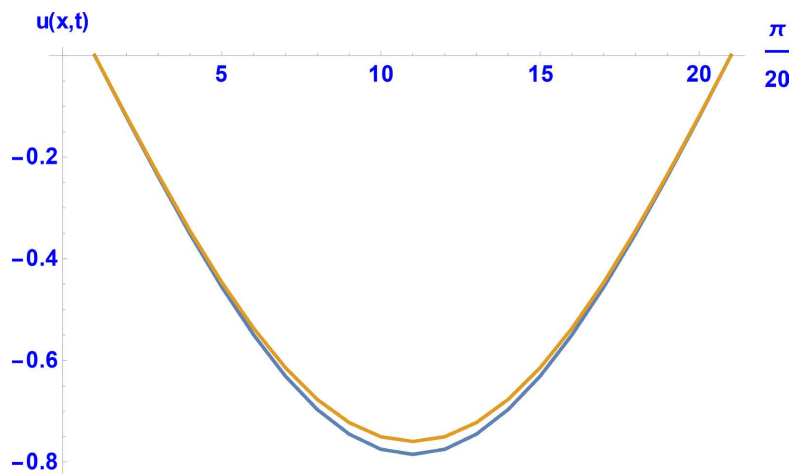


Figure 5. The exact and numerical results when the time $t = 15.0$ with $k = 0.01$.

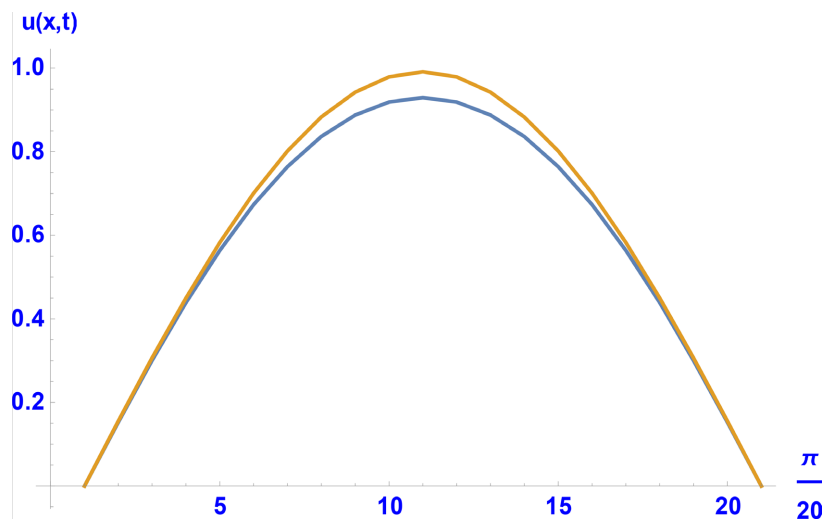


Figure 6. The exact and numerical results when the time $t = 25.0$ with $k = 0.01$.

From **Figures 5-9**, we observe that the smaller the $\Delta t = k$ (than the value of h), the better the accuracy. The numerical approximations are still acceptable within the large time.

The following figures, **Figures 10-13**, show the 3D representation of the numerical solutions of the dissipative equation for virus time and the same discretisations (h).

5. Conclusion

In this article, we discussed the non-polynomial spline method and the cubic

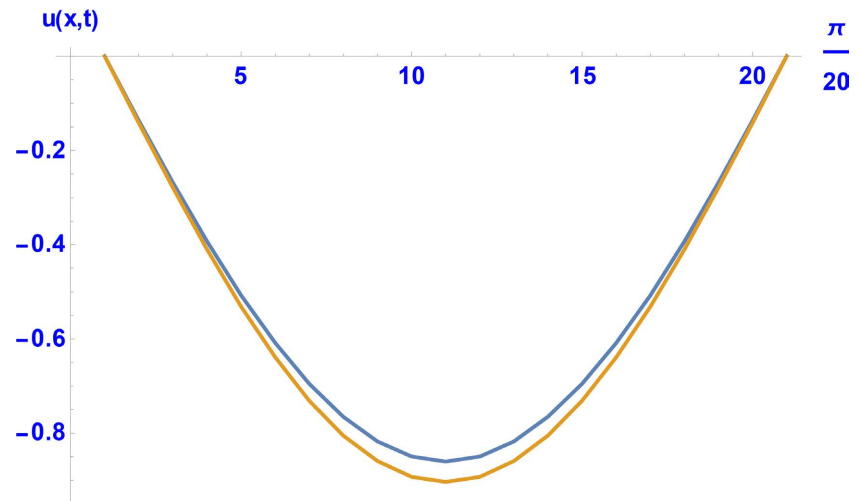


Figure 7. The exact and numerical results when the time $t = 35.0$ with $k = 0.01$.

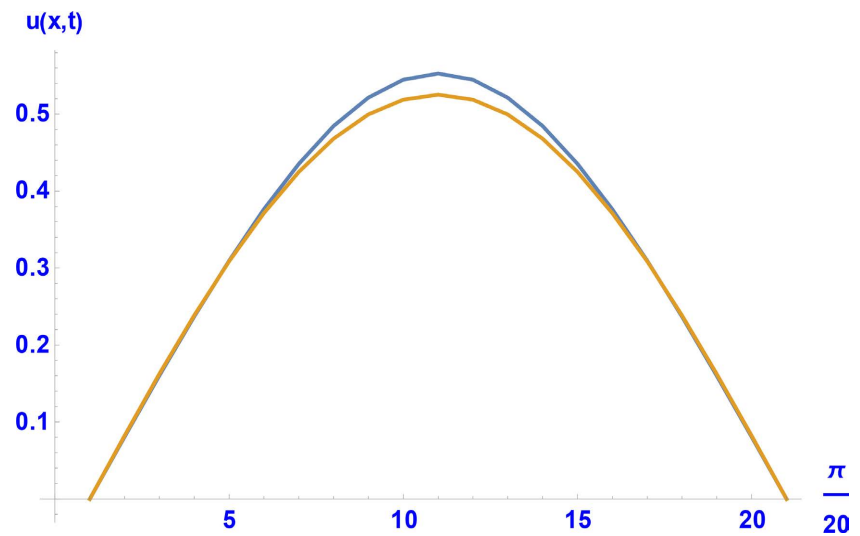


Figure 8. The exact and numerical results when the time $t = 45.0$ with $k = 0.01$.

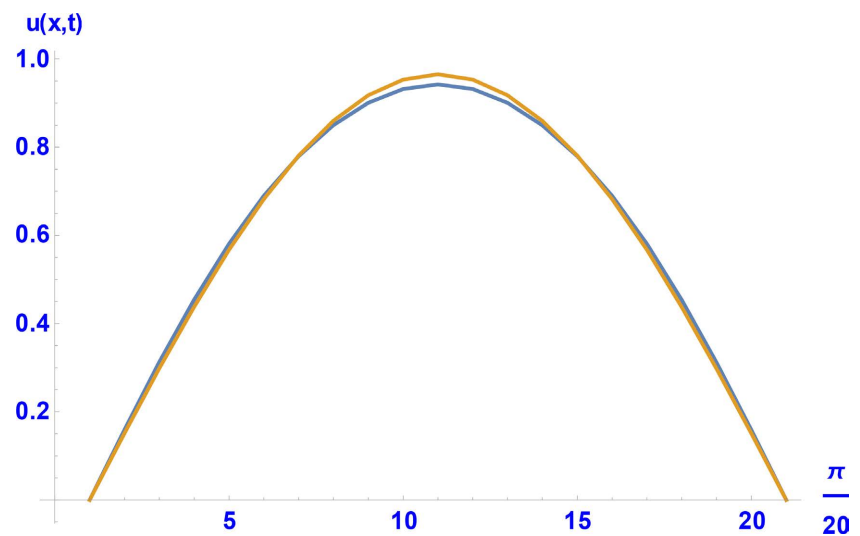


Figure 9. The exact and numerical results when the time $t = 50.0$ with $k = 0.01$.

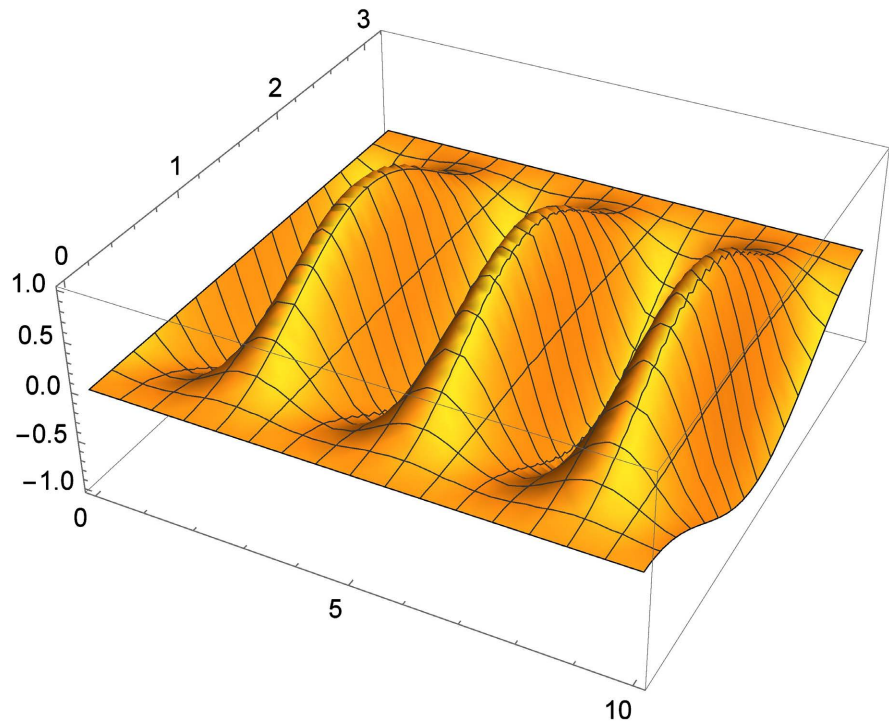


Figure 10. 3D representation of the numerical solutions of the dissipative from the time $t = 0.0$ to $t = 10.0$.

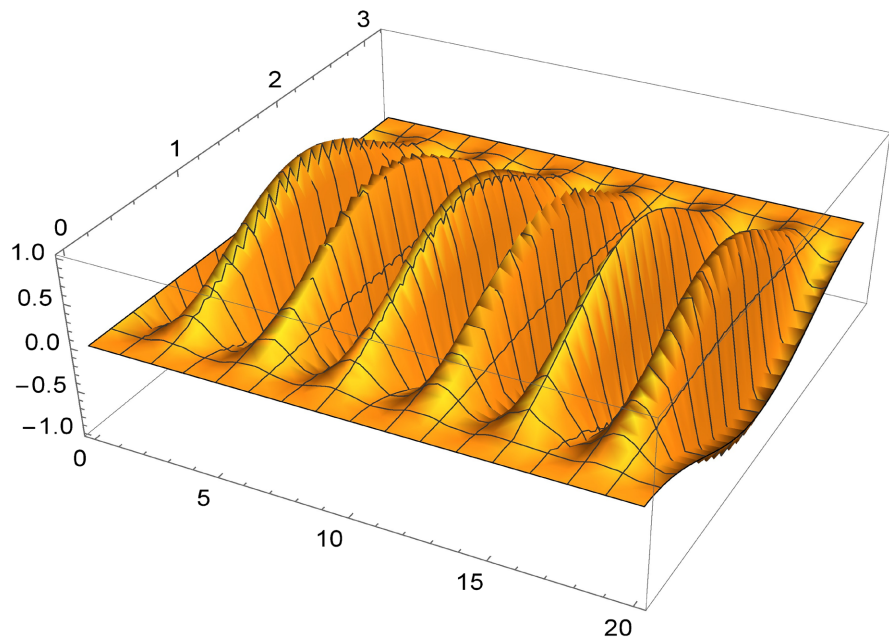


Figure 11. 3D representation of the numerical solutions of the dissipative from the time $t = 0.0$ to $t = 20.0$.

B-spline method for solving a nonlinear dissipative wave equation and its truncation errors. The stability analysis of these methods was shown to be conditionally stable. Furthermore, the obtained approximate numerical solutions maintain good accuracy compared with the exact solutions, especially for small values.

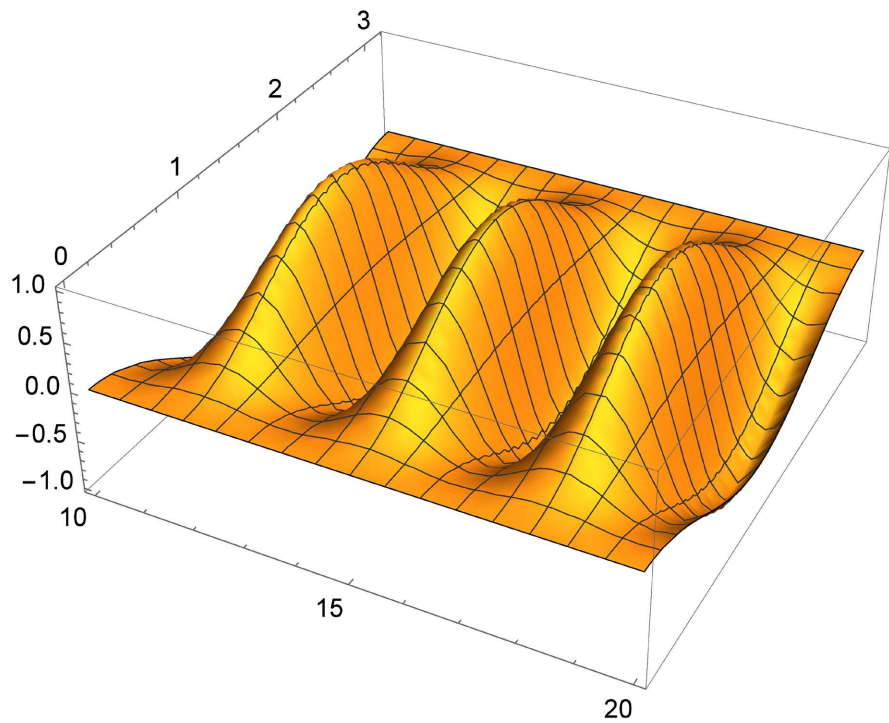


Figure 12. 3D representation of the numerical solutions of the dissipative from the time $t = 10.0$ to $t = 20.0$.

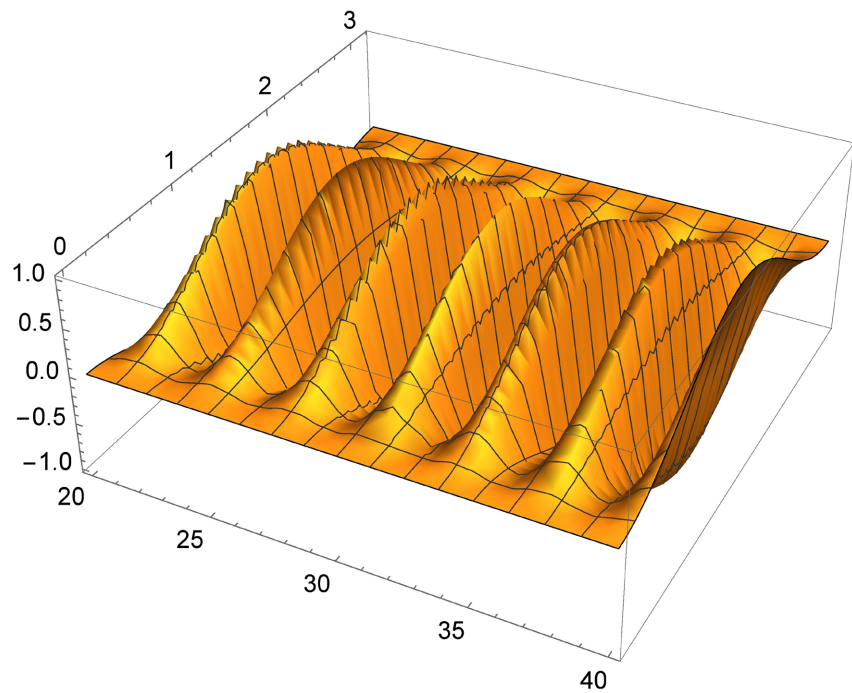


Figure 13. 3D representation of the numerical solutions of the dissipative from the time $t = 20.0$ to $t = 40.0$.

The results obtained by [4] demonstrate that solving the nonlinear dissipative wave equation using the cubic B-spline method is more accurate than using the non-polynomial spline method. A large set of values was used to treat the

nonlinear dissipative wave equation using the cubic B-spline method, and both 2D and 3D graph representations were provided. Our conclusion was that the non-polynomial spline method is more useful when the researcher wants to obtain the local truncation error, while the B-spline method is more accurate for solving nonlinear partial differential equations.

Conflicts of Interest

The authors declare no conflicts of interest regarding the publication of this paper.

References

- [1] Hereman, W. and Takaoka, M. (1990) Solitary Wave Solutions of Nonlinear Evolution and Wave Equations Using a Direct Method and MACSYMA. *Journal of Physics A: Mathematical and General*, **23**, 4805-4822. <https://doi.org/10.1088/0305-4470/23/21/021>
- [2] El Danaf, T.S. and Abdel Alaal, F.E.I. (2009) Non-Polynomial Spline Method for the Solution of the Dissipative Wave Equation. *International Journal of Numerical Methods for Heat & Fluid Flow*, **19**, 950-959. <https://doi.org/10.1108/09615530910994441>
- [3] Ahmed, Z., Ahmad, N., Ghonamy, M.I. and Rashid, N. (2020) On the Numerical Solution of the Dissipative Wave Equation at Midpoints. *Journal of Critical Reviews*, **7**, 8623-8632. <https://researchgate.net/publication/344467678>
- [4] Alaofi, Z., Sayed Ali, T. and Dragomir, S. (2021) A Numerical Solution of the Dissipative Wave Equation by Means of Cubic B-Spline Method. *Journal of Physics Communications*, **5**. <https://doi.org/10.1088/2399-6528/ac2940>
- [5] Adomian, G. (1994) Solving Frontier Problems of Physics: The Decomposition Method. Kluwer Academic Publisher, Boston, MA. <https://doi.org/10.1007/978-94-015-8289-6>
- [6] Amin, M., Abbas, M., Iqbal, M.K. and Baleanu, D. (2019) Non-Polynomial Quintic Spline for Numerical Solution of Fourth-Order Time Fractional Partial Differential Equations. *Advances in Difference Equations*, **2019**, 1-22. <https://doi.org/10.1186/s13662-019-2125-1>
- [7] Li, M., Ding, X. and Xu, Q. (2018) Non-Polynomial Spline Method for the Time-Fractional Nonlinear Schrödinger Equation. *Advances in Difference Equations*, **2018**, 1-15. <https://doi.org/10.1186/s13662-018-1743-3>
- [8] Adomian, G. (1994) Nonlinear Dissipative Wave Equations. *Applied Mathematics Letters*, **11**, 125-126. [https://doi.org/10.1016/S0893-9659\(98\)00044-5](https://doi.org/10.1016/S0893-9659(98)00044-5)